Weld HAZ Toughness and Its Improvement of Low Alloy Steel SQV-2A for Pressure Vessels (Report 2)†

– Microstructure and Charpy Impact Behavior of Intercritically Reheated Coarse Grained Heat Affected Zone (ICCGHAZ) –

Fukuhisa MATSUDA*, Kenji IKEUCHI**, Jinsun LIAO***
and Hiroki TANABE****

Abstract

Effects of peak temperature Tp_2 and cooling time $\Delta t_{8/5(2)eff}$ of the second thermal cycle on the impact properties and microstructures of ICCGHAZ during multi-pass welding were investigated in this study. ICCGHAZs were simulated with thermal/mechanical simulator Gleeble 1500. Microstructures were examined by optical microscopy, scanning electron microscopy (SEM) and transmission electron microscopy (TEM). The results showed that Charpy impact properties of ICCGHAZs were strongly influenced by the peak temperature Tp_2 and cooling time $\Delta t_{8/5(2)eff}$ of the second thermal cycle. For cooling time $\Delta t_{8/5(2)eff}$ of 6 s, the loss in impact value was observed over a narrow range of Tp_2, i.e. 973 - 1023 K, but for cooling time $\Delta t_{8/5(2)eff}$ of 40 s, the loss in impact value was observed over a wide range of Tp_2, i.e. 973 - Ac_3. For peak temperature Tp_2 in the range 923-1023 K, the loss in impact value was found to be due to the formation of M-A constituents in the interior of the grains and the necklace-like blocky structures along grain boundaries for both cooling times. However, for peak temperature Tp_2 higher than 1023 K, impact value was recovered in the case of 6 s because most of the prior structure was reaustenized and transformed into martensite, but the impact value was still low in the case of 40 s because upper bainite was formed upon cooling. It can be concluded from the results that M-A constituents in the interior of the grains and necklace-like blocky structures along grain boundaries impair the toughness of ICCGHAZ, and the toughness of ICCGHAZ is also affected by the microstructures of matrix.

KEY WORDS: (ICCGHAZ) (Impact Property) (Microstructure) (M-A Constituent) (Peak Temperature)

1. Introduction

Coarse grained heat affected zone (CGHAZ) of single-pass welded steels is generally known to have a lower toughness than other zones such as fine-grained heat-affected zone.[1-2] During multi-pass welding, CGHAZ of the first-pass weld is reheated by the subsequent thermal cycle. The intercritically reheated CGHAZ (ICCGHAZ), i.e. the region of first-pass weld CGHAZ reheated to austenite/ferrite two phase region (temperature range between Ac_1 and Ac_3), has been found to display lower toughness than even CGHAZ.[3] Because of this, many studies have been performed to find the cause of toughness loss of ICCGHAZ.[4-6]

According to these studies, the presence of the M-A constituent is mainly responsible for the loss in toughness. However, recent studies have shown that the loss in toughness is not solely due to this presence of the M-A constituent, but instead is usually associated with the distribution and morphology of the M-A constituent and the matrix microstructure.[7] It has also been suggested that the microstructure before intercritically reheating should be considered, in addition to the M-A constituent.[8]

Generally speaking, the toughness is determined by microstructures. With different peak temperature (Tp_2) of the second thermal cycle, the microstructure of ICCGHAZ is different. It is therefore important to study the effect of peak temperature Tp_2 on the microstructures. Moreover, although it has been known that the cooling rate (or cooling time) has a strong effect on the formation, morphology and distribution of the M-A

† Received on July 10, 1994

* Professor
** Associate Professor
*** Graduate Student
**** Graduate Student (Presently at Horiba Co., Ltd.)

Transactions of JWRI is published by Welding Research Institute, Osaka University, Ibaraki, Osaka 567, Japan

constituent in CGHAZ[10]), the effect of the cooling time $\Delta t_{8/5(2)}$ of the second thermal cycle on the property of the M-A constituent in ICCGHAZ is still unclear. Therefore, the purpose of this study is to investigate the effect of peak temperature Tp_2 and cooling time $\Delta t_{8/5(2)}$ of the second thermal cycle on the microstructures, the property of M-A constituents and the toughness in ICCGHAZ.

2. Experimental details

As in the previous paper, the experimental material was SQV-2A (0.19C-1.48Mn-0.62Ni-0.56Mo), a kind of low alloy steel for pressure vessels. The as-received steel was a quenched-and-tempered plate, and its thickness (t) was about 200 mm.

As shown in Fig. 1, samples (10x10x55 mm) for thermal cycle simulation were cut from the steel plate with the longest side parallel to the rolling direction at positions of 1/4t and 3/4t. Thermal/mechanical simulator Gleeble 1500 was employed to simulate the ICCGHAZs with different peak temperatures Tp_2 and cooling time $\Delta t_{8/5(2)eff}$ of the second thermal cycle. The simulated thermal cycles are shown in Figs. 2 and 3. The peak temperature of first thermal cycle Tp_1 was 1623 K; the holding time at the peak temperature was 6 s. Cooling time from 1073 to 773 K $\Delta t_{8/5(1)}$ of the first thermal cycle was designed to be 6 s, corresponding to low heat-input welding. Through the first thermal cycle, the CGHAZ was simulated. The microstructure of CGHAZ in this study was almost martensite, as shown in Fig.4. To simulate the ICCGHAZs with different peak temperatures, the peak temperature of the second thermal cycle Tp_2 was changed from 873 to 1173 K, covering the whole range of Ac_1-Ac_3. The holding time at the peak temperature of the second thermal cycle was also 6 s.

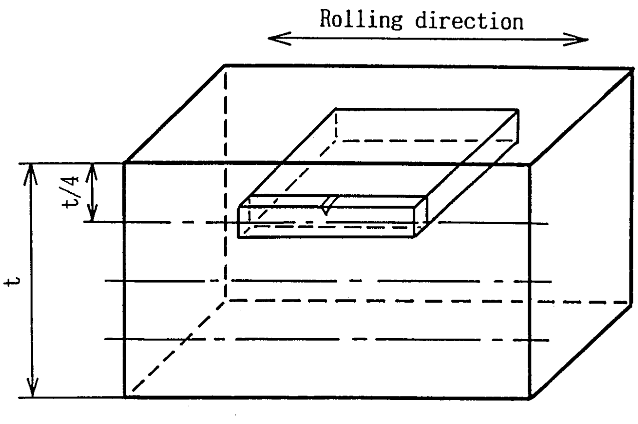

Fig. 1 Schematic diagram of samples

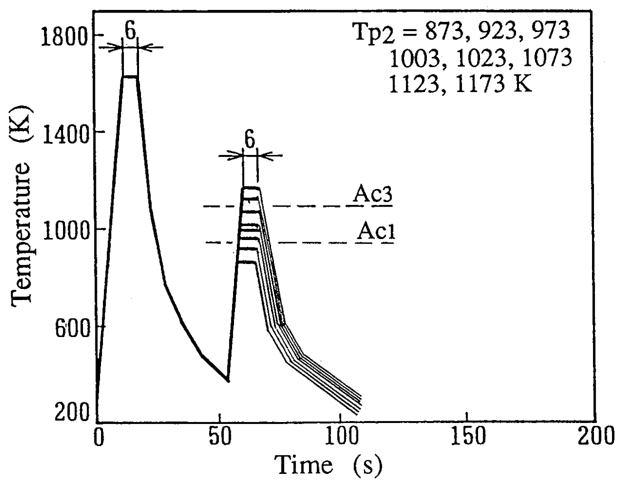

Fig. 2 Thermal cycles used for simulating ICCGHAZs ($\Delta t_{8/5(2)eff}$ = 6 s)

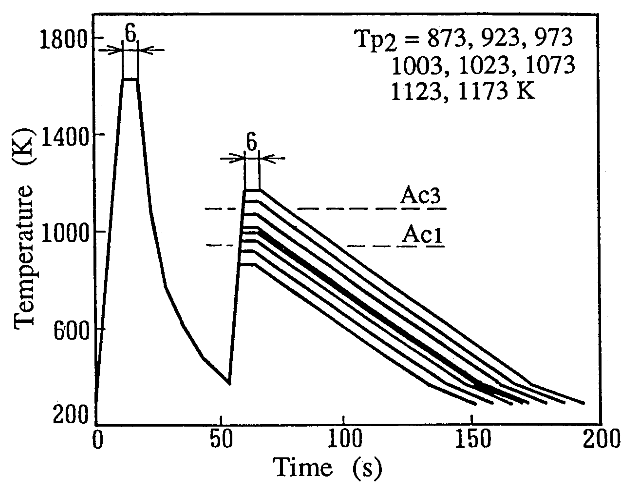

Fig. 3 Thermal cycles used for simulating ICCGHAZs ($\Delta t_{8/5(2)eff}$ = 40 s)

Ac_1 and Ac_3 temperatures of this steel during rapid heating were measured with a dilatometer attached to the Gleeble 1500 in this study. The Ac_1 temperatures of as-received material and CGHAZ were quite different and represented as Ac_1 and $(Ac_1)'$, respectively. In order to study the effect of the cooling rate on the microstructures and the property of the M-A constituent, the cooling times $\Delta t_{8/5(2)}$ of the second thermal cycle were chosen to be 6 and 40 s. Because the peak temperature Tp_2 could be lower than 1073 K (800 °C), the effective cooling time $\Delta t_{8/5(2)eff}$ was used instead of $\Delta t_{8/5(2)}$.

The thermal cycle simulated samples were machined with a standard V notch of 2 mm in depth, then subjected to the Charpy impact test at 293K in order to evaluate the toughness. For optical micrography, the polished specimen was etched in 3% Nital. In order to reveal the

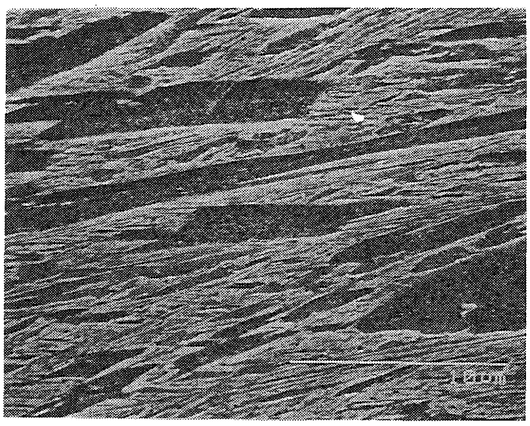

Fig. 4 Microstructure of CGHAZ

M-A constituent, a two-stage electrolytic etching method was used, by which ferrite and carbide would be etched preferentially in the 1st and 2nd stages respectively.[9] TEM technique was used to identify the M-A constituent and to reveal the more detailed microstructures.

3. Results and discussion

3.1 Impact behavior of ICCGHAZ

The absorbed energies of the Charpy impact test are shown in **Fig. 5** as a function of peak temperature Tp_2 of the second thermal cycle. The absorbed energy of the impact test was strongly influenced by the cooling rate for Tp_2 higher than 923K. For a high cooling rate ($\Delta t_{8/5(2)eff}$ = 6s), the absorbed energy was drastically decreased with the increasing of Tp_2 from 923 to 973K, whereas it recovered with further increasing of Tp_2 up to 1073K. For a low cooling rate ($\Delta t_{8/5(2)eff}$ = 40s), however, the absorbed energy was decreased with increasing of Tp_2 from 923 to 1073 K, and only a slight increase in absorbed energy was observed for Tp_2 higher than Ac_3. This difference in the effect of peak temperature Tp_2 on the absorbed energy can be attributed to the difference in microstructures formed during cooling at different cooling rates.

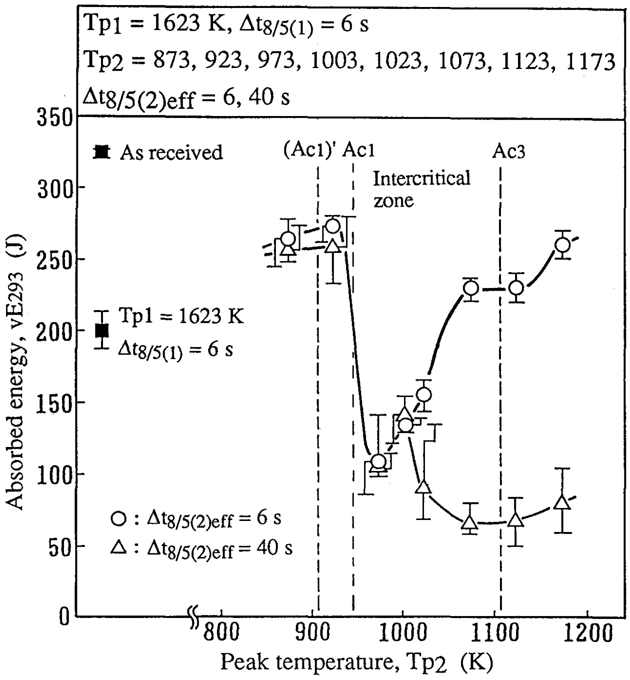

Fig.5 Absorbed energy of Charpy impact test as a function of peak temperature for both cooling times (Ac_1 for as received material; $(Ac_1)'$ for CGHAZ of SQV-2A)

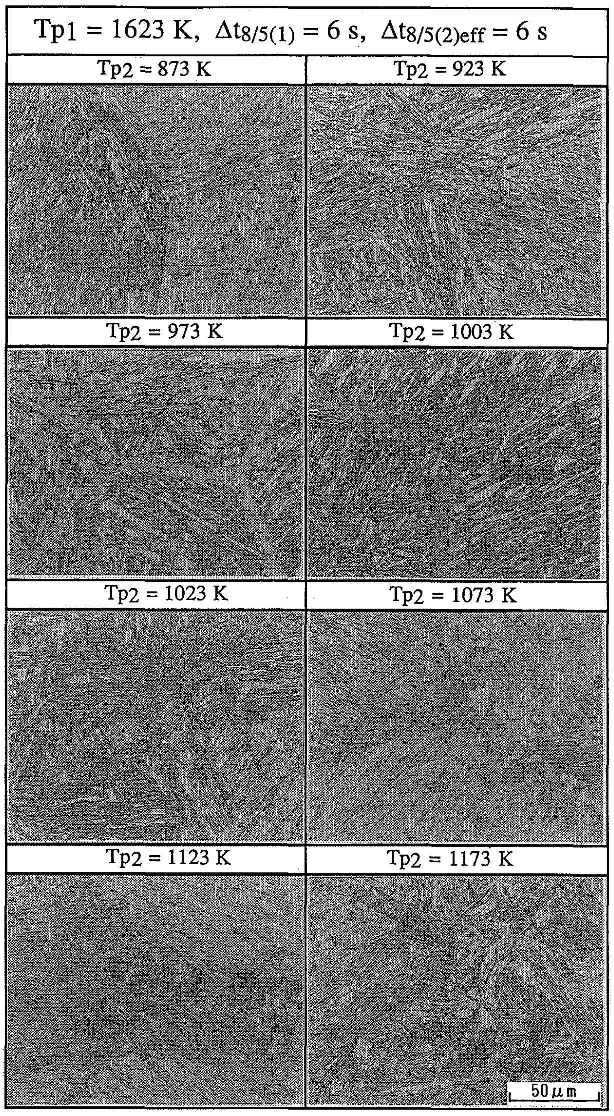

Fig. 6 Optical micrographs of ICCGHAZs ($\Delta t_{8/5(2)eff}$ = 6 s)

3.2 Effects of peak temperature and cooling time of the second thermal cycle on the microstructure of ICCGHAZ

The optical micrographs for cooling times $\Delta t_{8/5(2)eff}$ of 6 and 40 s are shown in **Fig.s 6** and **7** respectively. For $\Delta t_{8/5(2)eff}$ of 6 s, reaustenitization was observed to occur at prior austenite grain boundaries of CGHAZ when the peak temperature T_{p2} was over 923 K, but the microstructural changes in the interior of the grain could not be distinguished clearly by optical micrographs. For $\Delta t_{8/5(2)eff}$ of 40 s, the microstructural changes could be observed both at the prior austenite grain boundaries and within the grain.

The relation between Vickers hardness of ICCGHAZ and the peak temperature T_{p2} is shown in **Fig. 8**. For both cooling times, hardness was seldom changed for T_{p2}

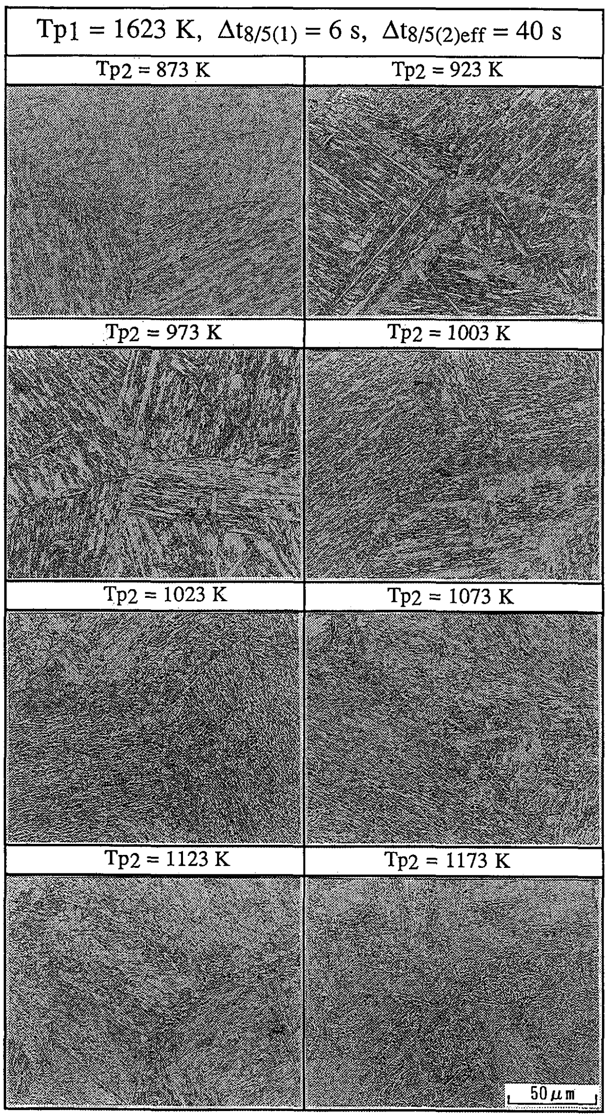

Fig. 7 Optical micrographs of ICCGHAZs ($\Delta t_{8/5(2)eff}$ = 40 s)

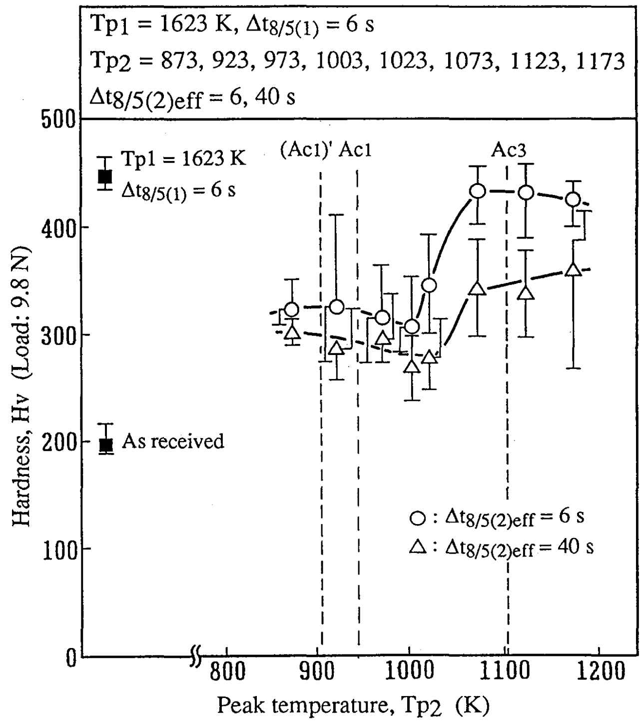

Fig. 8 Relation between hardness of ICCGHAZ and T_{p2}

from 923 to 1003 K, but above 1023 K, the hardness was increased. This implied that when the T_{p2} was higher than 1023 K, most of prior structures were reaustenized. During fast cooling, martensite was formed; but during slow cooling, structures consisting of bainite and martensite were formed, as shown later. The hardness of the martensitic structure or the complex structure of bainite and martensite was probably higher than that of a tempered martensitic structure, which might be the dominant structure for T_{p2} lower than 1023 K.

In order to reveal the M-A constituent and to observe the microstructural changes more clearly at high magnification, a two-stage electrolytic etching method together with SEM observation was employed. The micrographs are shown in **Fig.s 9** and **10** for $\Delta t_{8/5(2)eff}$ of 6 and 40 s respectively.

For cooling times $\Delta t_{8/5(2)eff}$ of 6 and 40 s, the peak temperature T_{p2} lower than $(Ac_1)'$ was insufficient to cause reaustenitization, so the M-A constituent could not be observed. Precipitated carbides were formed because of the tempering effect of the second thermal cycle on the martensitic structure of CGHAZ generated by the first thermal cycle, which resulted in superior toughness.

In the case of 6 s of $\Delta t_{8/5(2)eff}$, for peak temperatures T_{p2} in the range of 923 to 1003 K, bright structures, which are said to be M-A constituents,[9] were observed in the interior of the grains, and necklace-like

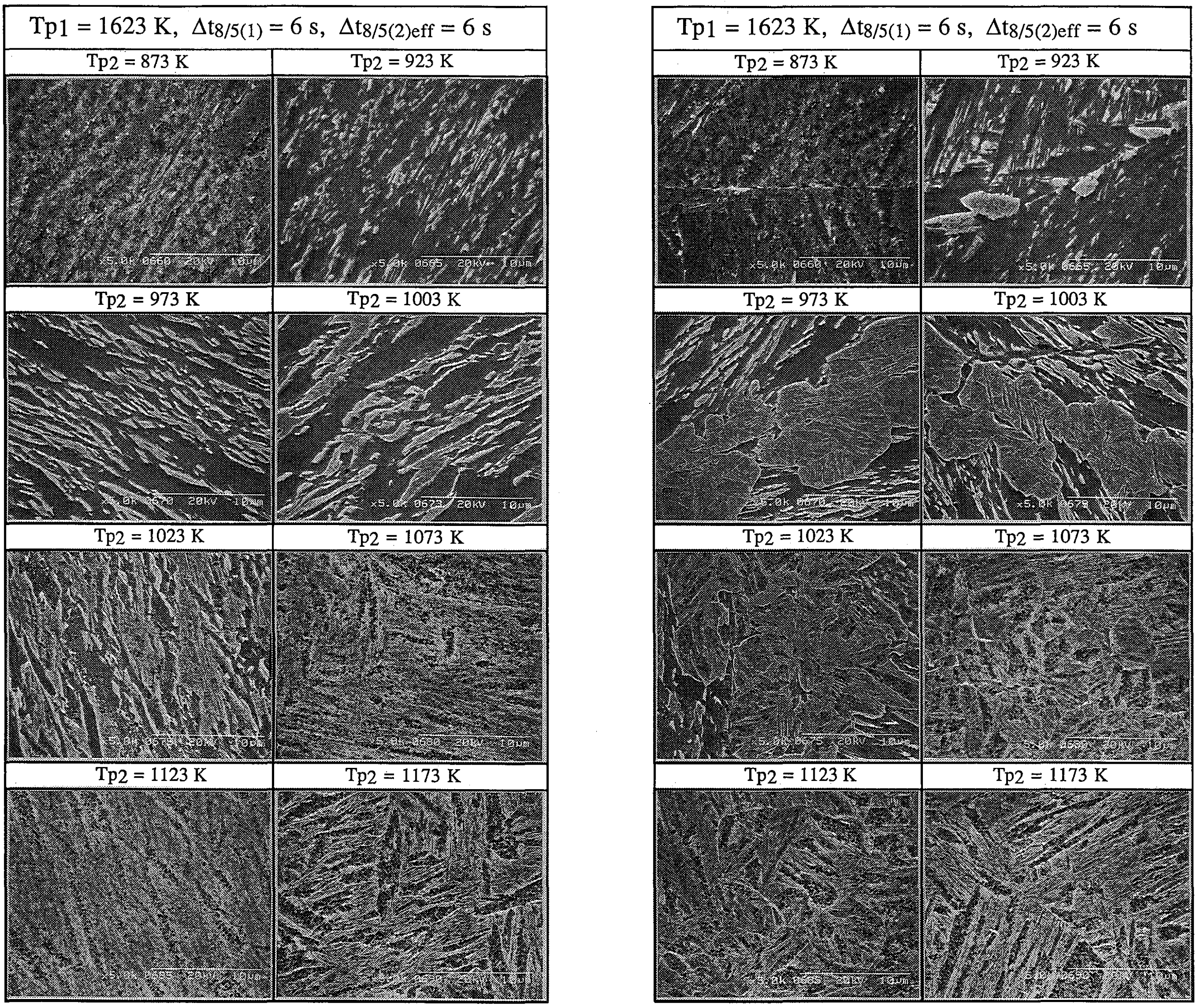

(a) The interior of the grain (b) Grain boundary area

Fig. 9 SEM micrographs of ICCGHAZs with Tp_2 from 873 to 1173 K ($\Delta t_{8/5(2)eff} = 6$ s)

blocky structures were formed at the grain boundary regions. In these blocky structures, high carbon martensite was observed, as shown in **Fig. 11**. For higher peak temperatures, for example Tp_2 from 1023 to 1123 K, reaustenitization occurred in a large area through the whole structure, and upon cooling at a high cooling rate, martensite was formed in the large area. At the same time, untransformed areas could also be observed as a dark area in the interior of grains. In untransformed areas, the prior structure was tempered by the second thermal cycle and carbides were precipitated. When reheated over Ac_3, prior structures were completely reaustenized and transformed to martensite again after being cooled at a high cooling rate, as shown in Fig. 9 .

In the case of $\Delta t_{8/5(2)eff}$ of 40 s, M-A constituents were formed in the interior of the grain for Tp_2 from 923 to 1023 K. For peak temperatures higher than 1073 K, reaustenitization occurred in a large area throughout the prior structure. On cooling, this resulted in the microstructures of upper bainite, lower bainite and a little martensite because of the low cooling rate, as shown in Fig. 10 (a).

The necklace-like blocky structures were also formed at the prior grain boundaries for peak temperatures Tp_2 from 923 to 973K in the case of $\Delta t_{8/5(2)eff}$ 40s, but with further increasing of Tp_2, the reaustenitized area near the prior grain boundary became larger. These austenite blocks were decomposed to M-A constituents and carbides

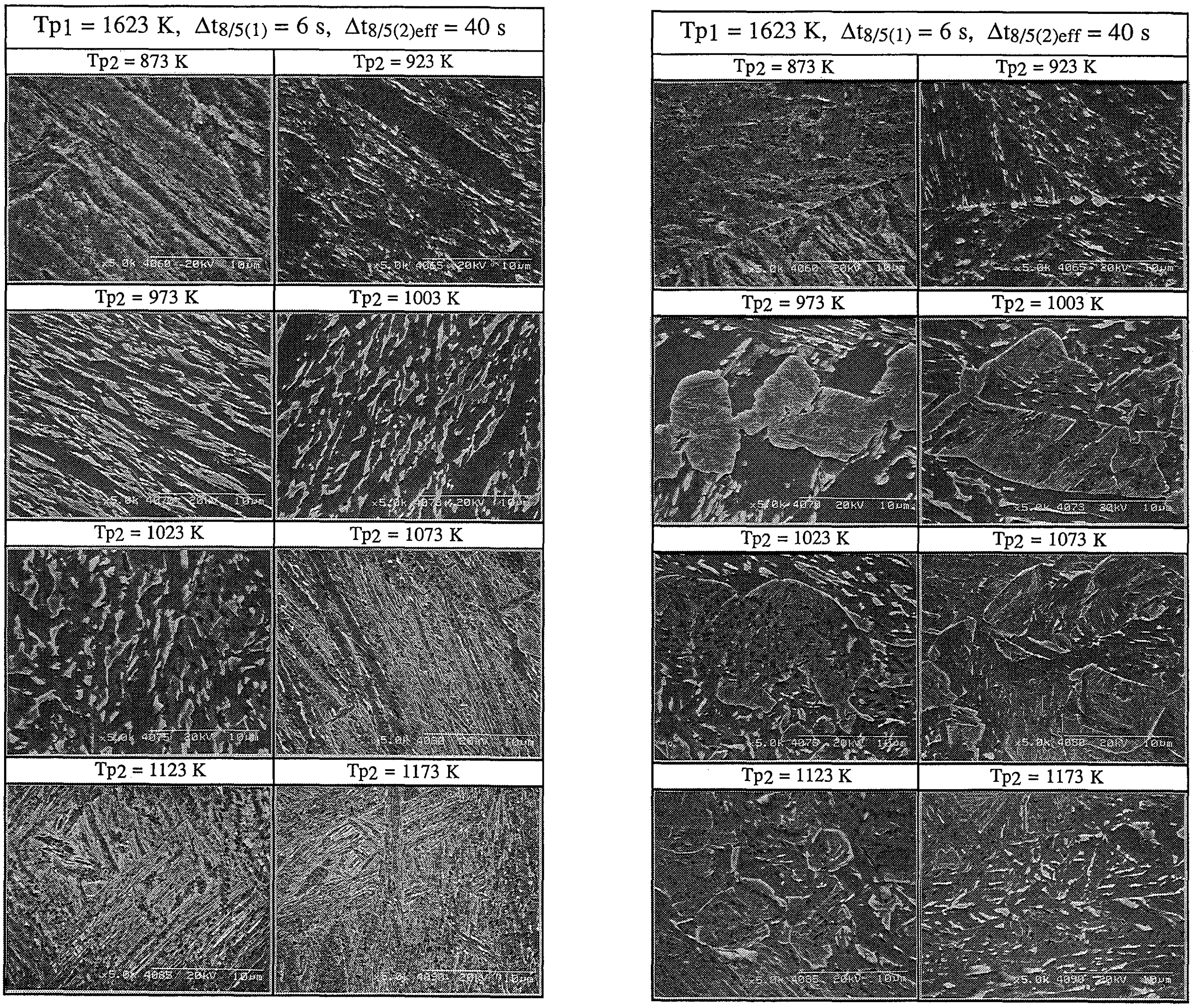

(a) The interior of the grain (b) Grain boundary area

Fig. 10 SEM micrographs of ICCGHAZs with Tp_2 from 873 to 1173 K ($\Delta t_{8/5(2)eff}$ = 40 s)

instead of forming blocky structures, as shown in Fig. 10 (b).

3.3 Effect of cooling time $\Delta t_{8/5(2)eff}$ on the M-A constituent

The bright structures revealed by two-stage electrolytic etching were identified by TEM technique. For $\Delta t_{8/5(2)eff}$ of 6 s, island-like martensite with high dislocation density was observed in bright structures, as shown in **Fig. 12 (a)**. A twin image, which has been observed in the M-A constituent by several researchers,[11] could not be found in this case. Particle-like carbides were observed in the areas not reaustenized, as shown in **Fig. 12 (b)**. This confirms the tempering effect of the second thermal cycle. For $\Delta t_{8/5(2)eff}$ of 40 s, twin martensite was observed in the bright structures, as shown in **Fig. 13**. Although we failed to find the retained austenite by TEM observation and electron diffraction, the retained austenite could be detected by X-ray diffraction analysis.

The difference in the M-A constituent suggests that the carbon content of the M-A constituent depends on cooling time $\Delta t_{8/5(2)eff}$. Although the reason has not still been understood clearly, this result is supported by the micro-hardness measurement of the blocky structure. It can be seen from **Fig. 14** that the blocky structures in

Fig. 11 TEM micrograph of the blocky structure

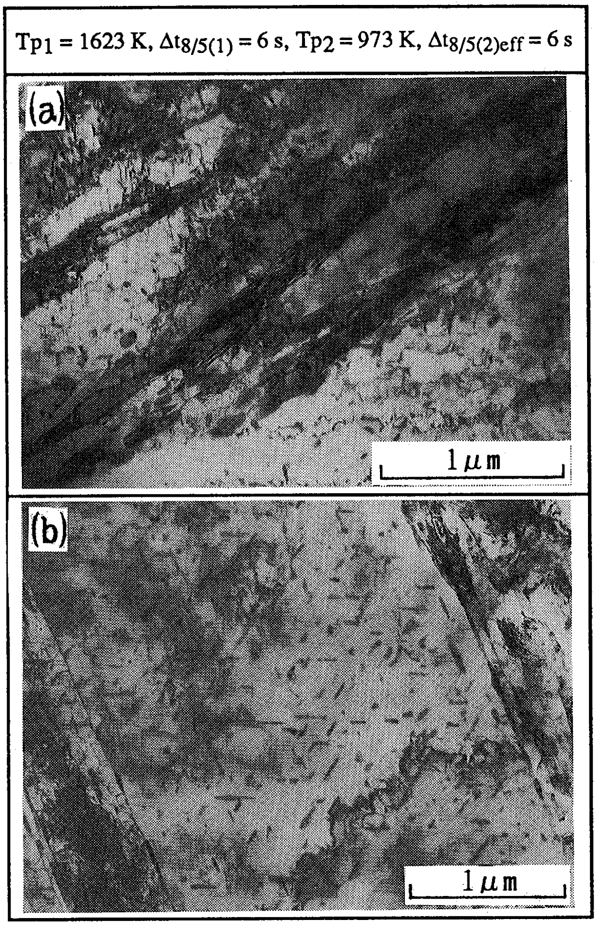

Fig. 12 TEM micrographs in the interior of the grain ($\Delta t_{8/5(2)eff} = 6$ s)

the case of 40 s are slightly harder than those in the case of 6 s at the same peak temperatures Tp_2 of 923 and 973K.

Of course, the peak temperature Tp_2 also has an effect on the carbon content of the M-A constituent. With increasing Tp_2, the carbon content of the reaustenized region will become lower, according to the phase diagram. Therefore, the carbon content of the M-A constituent is probably higher at low Tp_2 than high Tp_2. Because of this, the carbon content of blocky structures becomes lower with increasing Tp_2. When Tp_2 is higher than 1003 K, the blocky structure is decomposed into bainite and small M-A constituents during cooling at a low cooling rate ($\Delta t_{8/5(2)eff} = 40$ s).

3.4 Factors affecting toughness

From the experimental results and microstructural analysis mentioned above, it can be concluded that M-A constituents in the interior of grains and blocky structures at grain boundaries may be the reasons for the loss of toughness because of their high hardness.

For $\Delta t_{8/5(2)eff}$ of 6 s, the toughness is greatly lost for a peak temperature in the range of 973 to 1023 K. At these peak temperatures, M-A constituents form in the interior of grains in a large amount, and necklace-like blocky structures form at the grain boundaries. For $\Delta t_{8/5(2)eff}$ of 40 s, the loss in toughness for peak temperature Tp_2 from 973 to 1003 K can also be concluded to be due to the formation of M-A constituent within the grains and the blocky structures at the grain boundaries.

From the observation of microstructures near the fracture surface, it can be seen that microcracks initiate between the blocky structure and matrix, and propagate into the interior of the grain, or along the grain boundary, as shown in **Fig. 15**. Therefore, it can be concluded that the formation of blocky structures at the grain boundaries is one of the main reasons for the loss in toughness. But from a fractograph, it can be seen that intra-grain cleavage fracture is predominant, and there is just a little fracture along grain boundaries. In addition, the M-A constituent

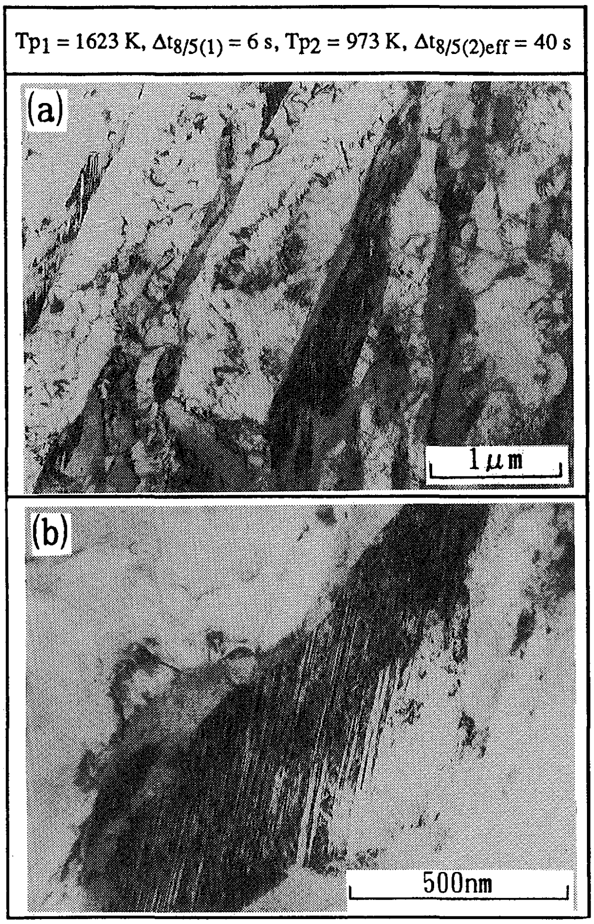

Fig. 13 TEM micrographs in the interior of the grain ($\Delta t_{8/5(2)eff}$ = 40 s)

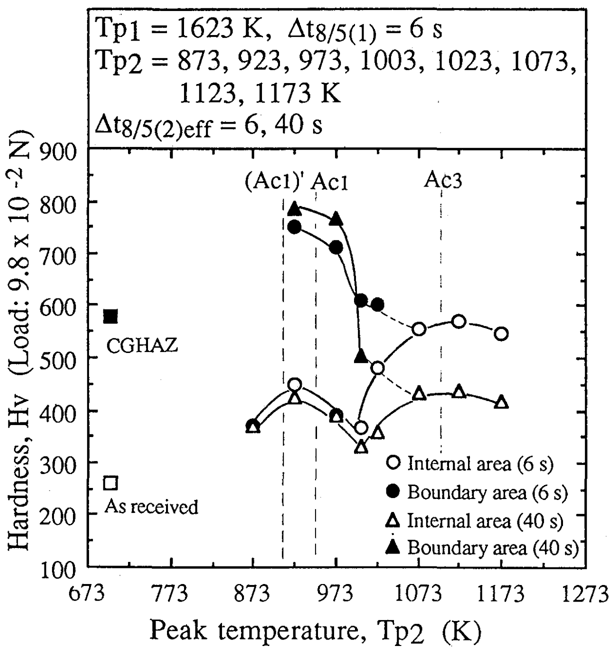

Fig. 14 Relation between micro-hardness and Tp_2

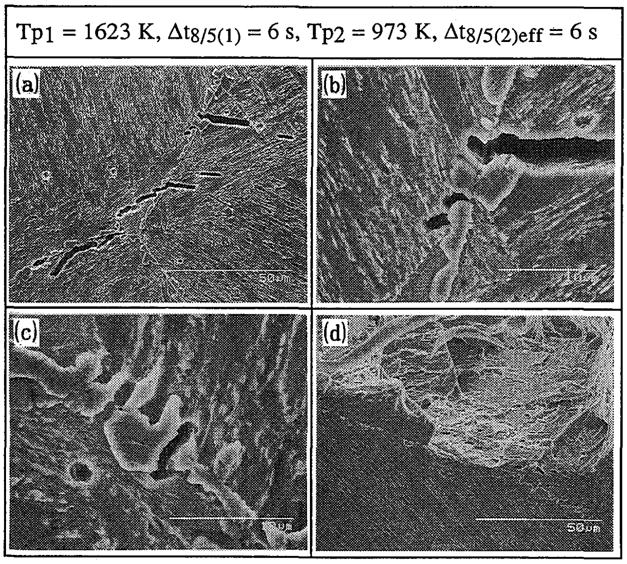

Fig. 15 Microcracks near grain boundary ((a) showing microcracks near grain boundaries; (b) and (c) showing that microcracks initiate between blocky structure and matrix; (d) showing cleavage fracture along grain boundary)

has been found to impair the toughness of CGHAZ as mentioned in the previous report.[10] Therefore, the M-A constituent in the interior of grains also seems to be responsible for the loss in toughness of ICCGHAZ.

However, the toughness may also be closely related to the matrix. For the peak temperature of 923 K, the very small M-A constituent and blocky structures can be observed in the interior of grains and at the grain boundaries respectively, but most of structures are tempered martensite which is said to have superior toughness. So the toughness is still high even though the M-A constituent has been formed. Furthermore, for the peak temperatures Tp_2 higher than 1023 K, most of the prior structure is reaustenized, and transformed into martensite in the case of fast cooling, so that the toughness is recovered. But in the case of slow cooling, reaustenized areas are transformed mostly into upper bainite, so the toughness can not be recovered.

4. Conclusions

The martensitic structure of CGHAZ generated by the first thermal cycle was intercritically reheated during the second thermal cycle. The effects of peak temperature Tp_2 and cooling time $\Delta t_{8/5(2)eff}$ of the second thermal cycle on the microstructure, M-A constituent and toughness in the ICCGHAZ have been investigated. The main conclusions are as follows:

(1) Charpy impact properties of ICCGHAZ were strongly influenced by peak temperature Tp_2 and cooling time $\Delta t_{8/5(2)eff}$ of the second thermal cycle. For cooling time $\Delta t_{8/5(2)eff}$ of 6 s, the loss in absorbed energy was observed over a narrow range of Tp_2. For SQV-2A steel, this temperature range was 973 - 1023 K. For cooling time $\Delta t_{8/5(2)eff}$ of 40 s, however, the loss in absorbed energy was observed over a wide range of Tp_2, i.e. 973 K - Ac_3.

(2) For peak temperature Tp_2 in the range 923-1023 K, M-A constituents were formed in the interior of the grains, and blocky structures were formed along grain boundaries for both cooling times. When Tp_2 was higher than 1023 K, most of the prior structure was reaustenized and transformed to martensite again for $\Delta t_{8/5(2)eff}$ of 6 s, or for $\Delta t_{8/5(2)eff}$ of 40 s transformed to upper bainite, M-A constituents and a little lower bainite and martensite.

(3) For peak temperature Tp_2 at 973 K, twin martensite was observed in the M-A constituent for $\Delta t_{8/5(2)eff}$ of 40 s, but no twin was observed for $\Delta t_{8/5(2)eff}$ of 6 s.

(4) The hard blocky structures along grain boundaries and the M-A constituents in the interior of the grains were responsible for the loss in absorbed energy for Tp_2 in the range 973 - 1003 K. For Tp_2 higher than 1003 K, absorbed energy increased in the case of 6 s of $\Delta t_{8/5(2)eff}$ because most of the prior structure was reaustenized and transformed to martensite again, whereas absorbed energy was still low in the case of 40 s of $\Delta t_{8/5(2)eff}$ because the upper bainite and M-A constituents were formed.

Acknowledgment

Thanks are due to Dr. Y. Kikuchi and Dr. T. Kuroda for their helpful discussion.

References

1) Makoto SATO and Kazunari YAMATO, "On the Microstructure and Toughness of HAZ in as rolled or Normalized 50 and 60 Kg/mm2 High Strength Steel", Journal of Japan Welding Society, Vol. 50, No. 1 (1981), pp. 11-19 (in Japanese).
2) Junichiro TSUBOI and Yukio HIRAI, "Microstructure and Toughness of Weld Heat Affected Zone in Quenched-Tempered High Strength Steels", Journal of Japan Welding Society, Vol. 50, No. 1 (1981), pp. 28-37 (in Japanese).
3) Y. Nakao et al., "Distribution of Toughness in HAZ of Multi-pass Welded High Strength Steel -Study on Distribution of Microstructure and Toughness in Multi-pass Weld HAZ (Report 2)-", Quarterly Journal of the Japan Welding Society, Vol. 3, No. 4 (1985), pp. 99-107 (in Japanese).
4) B.C. KIM, S. LEE, N.J. KIM, and D. Y. LEE, "Microstructure and Local Brittle Zone Phenomena in High-Strength Low Alloy Steel Welds", Metallurgical Trans. A, Vol. 22A, Jan. 1991, pp. 139-149.
5) C.L. Davis and J.E. King, "Effect of cooling rate on intercritically reheated microstructure and toughness in high strength low alloy steel", Materials Science and Technology, Jan. 1993, Vol. 9, pp. 8-15.
6) V.M. Linton and J.E. King, "The Effect of Heat Input on the Heat Affected Zone Toughness of Two Offshore Steels", Proceeding of the 3rd International Conference on Trend in Welding Research, Gatlinburg, Tennessee, USA, June 1-5, 1992, pp. 345-349.
7) C.L. Davis and J.E. King, "Cleavage Initiation in the Intercritically Reheated Coarse-Grained Heat-Affected Zone: Part 1. Fractographic Evidence", Metallurgical Trans. A, Vol. 25A, March 1994, pp. 563-573.
8) T. Shiwaku et al., "Metallurgical Factors on Toughness in Intercritically Reheated HAZ of Low-C Low-Alloy Steel", Bulletin of Annual Meeting of Japan Welding Society, Vol. 54 (1994-4), pp. 240-241 (in Japanese).
9) Hiroshi IKAWA et al.., "Effect of Martensite-Austenite Constituent on HAZ Toughness of a High Strength Steel", IIW Doc. IX-1156-80.
10) F. MATSUDA, K. IKEUCHI and J. LIAO, "Weld HAZ Toughness and Its Improvement of Low Alloy Steel SQV-2A for Pressure Vessels (Report 1) -Effect of Cooling Time on Microstructure and Charpy Impact Value in Single Thermal Cycle-", Trans. of JWRI, Vol. 22, No. 2 (1993), pp. 271-279.
11) Metallographic Atlas of Steel, Special Alloy Steel and Non-ferrous Metal Welds, Edited by Japan Welding Society, 1984.